PSFC/JA-08-26

Real-time Fast Ferrite ICRF Tuning System on the Alcator C-Mod Tokamak

Lin, Y., Binus, A., Wukitch, S. J.

August 2008

Plasma Science and Fusion Center
Massachusetts Institute of Technology
Cambridge MA 02139 USA

Real-time Fast Ferrite ICRF Tuning System on the Alcator C-Mod Tokamak

Y. Lin[*], A. Binus, S. J. Wukitch

Plasma Science and Fusion Center, Massachusetts Institute of Technology, Cambridge, MA 02139, USA

Abstract

A real-time ion cyclotron range of frequencies (ICRF) antenna matching system has been successfully implemented on Alcator C-Mod. This system is a triple-stub tuning system working at 80 MHz, where one stub acts as a pre-matching stub and the other two stubs use fast ferrite tuners (FFT) to accomplish fast tuning. It utilizes a digital controller for feedback control (200 μs per iteration) using real-time antenna loading measurements as inputs and the coil currents to the FFT as outputs. The system has achieved and maintained matching for a large range of plasma parameters, including L-mode, H-mode, and plasmas with edge localized modes. It has succeeded in delivering up to 1.85 MW net rf power into H-mode plasmas at max voltage of 37 kV on the unmatched side of the matching system.

Keywords: ICRF, matching, ferrite tuner, real-time, Alcator C-Mod tokamak

---

[*] Correspondent author: Yijun Lin, email: ylin@psfc.mit.edu

1. Introduction

Ion cyclotron range of frequencies (ICRF) heating has been a major auxiliary heating tool in tokamaks, and it will be applied in ITER as the main bulk ion heating method. An ICRF system typically consists of an rf generator, transmission line network, and antenna. The antenna input and generator output impedance are mismatched and the situation is further complicated by the fact that the antenna impedance is largely reactive and varies with plasma conditions. To maintain efficient power transfer, the matching network needs to transform the antenna impedance to the generator impedance and follow the loading variation to isolate the generator from the load variation.[1] Traditionally, the matching in this frequency range (20-120 MHz) is achieved by length-variable short stubs, phase shifters (trombone stretchers), and tunable or fixed vacuum capacitors. However, because the antenna loading varies with plasma parameters, for example, the plasma confinement changes from L-mode to H-mode, and during edge localized mode (ELM) activities, a fixed (or tunable between-shot) matching network may not be sufficient in maintaining the matching throughout the entire plasma discharge. The high voltage-standing-wave-ratio (VSWR) caused by such mismatch can reduce the maximum power output available from the generator, and can also force the generator protection system to shut off the generator unnecessarily assuming that an arc in the transmission line has occurred. Therefore, a matching system that adjusts the matching network following the antenna loading variation in real-time is desirable to maximize the generator power, raise the rf power utilization rate, and improve experimental flexibility by allowing the antenna to be matched throughout a large range of plasma parameters.

Several methods have been developed and implemented on various magnetically-confined fusion devices for real-time matching, including plasma position control [2,3], varying frequency [4], conjugate-T networks [5], motorized vacuum capacitors [6,7], and liquid stubs [8, 9, 10]. A survey of fast matching techniques is discussed in Refs. [1] and [11]. On Alcator C-Mod, various constraints and experimental results have guided our selection of the method to do real time matching. Position control has been tested previously with limited success. Recent work has shown that the antenna loading variation on Alcator C-Mod is dominated by the height of the pedestal while the distance to the cut-off layer only contributes for about 20%.[12] Modifying the plasma position to maintain low VSWR often interferes with experimental demands. Utilizing the generator bandwidth to follow the load changes is also ineffective because the Alcator C-Mod ICRF system has too narrow a frequency bandwidth for the relatively short transmission line length. We have also investigated conjugate-T based matching network but found that the system did not provide load tolerance due to the strong coupling between antenna elements [13]. A system based on dielectric liquid stubs has been considered but the time response (~ seconds) of this scheme is far too slow to be applicable for Alcator C-Mod plasmas (< 5 sec plasma pulse) [14]. To accomplish a response time in milliseconds or shorter, advanced tuners utilizing low loss soft ferromagnetic materials (ferrite) can be used with no moving part. Fast ferrite tuners (FFTs) have been used previously on DIII-D [15], ASDEX-upgrade [16,17,18], and are being developed for KSTAR [19]. On Alcator C-Mod, we have successfully developed and implemented a FFT-based triple-stub real-time matching system. The system on Alcator C-Mod has coupled 1.85 MW net rf power, and maintained antenna matching in a large plasma parameter space.

In this paper, we will report the design and performance of this FFT system. In Section 2, the design of the FFT system is described. Section 3 reports the system performance in different plasma conditions, including L-mode, H-mode and ELMs. The rf power loss during high power operation for a previous double-stub configuration is also discussed followed by discussion and summary in Section 4.

2. Design of the real-time FFT system

The ICRF system on Alcator C-Mod includes three antennas [20] and the FFT system is installed in the transmission network of the E ICRF antenna (operated at 80 MHz). The first installation, in 2007, was a double-stub system as described briefly in Refs. [21] and [22]. In this paper, we report an upgraded triple-stub system. Fig. 1 shows the layout of the real-time FFT system. Stub 1 and 2 are ferrite tuners and stub 3 is a pre-matching stub that lowers the rf voltage on the ferrite tuners. Excellent matching has been achieved and maintained through real-time digital feedback. We describe the system in detail in the following sections.

2.1 Triple-stub matching method

In Fig. 2, the principle of the triple stub tuning method [23] is shown on a Smith chart with normalized admittance coordinates, $Y = G + jB$, where Y is the complex admittance, G is the conductance and B is the susceptance. A lossless stub adds only the susceptance, thus it moves the admittance along the constant conductance G circles. A straight

transmission line moves the admittance along the equal VSWR circles. The complex

voltage reflection coefficient, $\Gamma = (1\text{-}Y)/(1\text{+}Y)$, can be obtained from the horizontal (-

$Re(\Gamma)$) and vertical labels (-$Im(\Gamma)$) of the Smith chart. In Fig. 2, an antenna loading that

induces a Γ at the physical location P6 in Fig. 1 is transformed to point P5 through stub 3,

and to P3 via stub 2, then to P1 via stub 1 toward the generator. A perfect matching can

be achieved at P1, that is, from location P1 to the generator, we have $\Gamma = 0$ and $Y=Y_0$, or

equivalently, impedance $Z = Z_0 = 50$ ohm, the characteristic impedance of the coaxial

line. In principle, a triple-stub configuration can match to any antenna loading, but due to

the limitation of the total variable electrical lengths in the ferrite tuners (see Section 2.2),

the Alcator C-Mod system is designed to cover the range of the E antenna loading for

most plasmas.

2.2 Fast ferrite tuners

The ferrite tuners (transmission line sections filled with ferrite material) were made by

Advanced Ferrite Technologies in Germany and designed for 60 MHz (specifications can

be found in Ref. [18]). In general, ferrite materials need to work at high magnetization to

minimize rf loss. In these tuners, the horizontally laid ferrite tiles are magnetized by a

permanent biasing vertical field at approximately 0.016 T. For ferrite material at nearly

saturated magnetization M_0, its permeability varies approximately following $\mu \sim M_0/H$,

where H is the strength of applied magnetic field. As a result, varying H around the

biasing field can modify the effective permeability of the tuner, and change the rf wave

phase velocity, which is proportional to $1/\mu^{1/2}$. For instance, by reducing the external

magnetic field, we can increase the effective μ, reduce the phase velocity and shorten the

rf wave wavelength, which results in longer equivalent electrical length of the tuner. The

requirement of low loss (i.e., adequate biasing field) sets an upper limit of μ that a system

can change. Inside each tuner, we use two current coils (24 turns each) above and below the ferrite tiles to generate the varying field, approximately perpendicular to the ferrite material. The power supply can provide current ranging from -150 A to 150 A resulting in the variable field in the range of approximately +90 Gauss to -90 Gauss. The electrical length at 80 MHz as measured by a network analyzer is shown to change from -12 cm to 24 cm relative to zero current in the coils. This range is shorter than the 1/4 λ variation at 60 MHz reported in the design document. Because of the power supply limitation in driving large inductance, the coil current can only be varied at a rate up to 75 A/ms, corresponding to ~9 cm/ms in terms of the equivalent electrical length.

The stubs' maximum electrical lengths determine the operation region of the matching system. In Fig. 2, we show on a Smith chart the admittance region that the FFT system can make perfect match without railing the power supply, and also show the admittance range that with one or both currents railed, the region that the system can transform the antenna loading at location P6 to within power reflection $|\Gamma|^2 < 25\%$ (VSWR = 3) at location P1.

The ferrite material is a relatively poor thermal conductor and its losses increase with ferrite temperature and local rf current. The center conductor and the ferrite tiles are water cooled, and the inlet and outlet water temperatures are built into the operation interlock. The tuners are filled with 2 bar of SF6 to obtain reliable high voltage operation, and equipped with optical arc detectors to directly monitor the tuners for fast rf shut-off.

2.3 Real-time Control system

The real-time feedback control system is based on the architecture of the Alcator C-Mod plasma control system [24], and the feedback control is achieved via a Linux server, 32-input/16-output digitizer, and MDSplus data system [25]. Directional couplers (DC1, DCC, DC2, and DC3 in Fig. 1) measure the forward power, reflected power, and phase at four different locations on the transmission line. The computer runs at 200 μs iterations, and at the start of the iteration, the computer converts the directional coupler measurements to the local complex voltage reflection coefficient Γ and calculates the required stub lengths to get perfect match. Then the computer determines the coil currents for the tuners, and sends out the control signals to the tuner power supplies at the end of computation. The computation times at different scenarios are always shorter than 150 μs when interrupts to the server are disabled during the pulse. A more detailed description of the control system can be found in Ref. [21].

3. Performance of the real-time FFT system

In this section, we report the performance of the FFT system in various plasma discharges, including L-mode, H-mode, and ELMs. We also discuss the rf power loss observed on the tuners in the previous double-stub design when the circulating rf power in the system was very high.

3.1 Performance in L-mode and Enhanced D_α H-mode

The antenna loading in H-mode is much smaller than that in L-mode mainly because of the steepened plasma density profile in the pedestal region [12,26]. In Fig. 3-(a), we plot the antenna loading together with the D_α trace in a typical plasma discharge in L-mode and during enhanced D_α H-mode. The antenna loading is defined as the equivalent loading resistance on the unmatched line, $R_c = Z_0/S$, and $S = (1+|\Gamma|)/(1-|\Gamma|)$ is the

VSWR. In this discharge, the plasma entered H-mode at 0.65 sec heated by total ~3 MW ICRF power (the E antenna contributes ~1 MW). The antenna loading changed suddenly at this transition from about 12 ohm to 7 ohm. During the H-mode period, the loading evolved with the plasma condition, which is evident in the correlation between the loading and the D_α trace. In 3-(b), the forward rf power and reflected rf power measured by directional coupler DC1 (see Fig. 1) is plotted. The coil currents on the tuners are shown in panel 3-(C). Less than 10 kW (<1%) reflected power out of 1 MW forward power was maintained during L-mode and H-mode periods under the feedback from the FFT. At the L-H transition, the reflected power rose because of the sudden loading change, but the feedback system was able to reduce it to below 1% in less than 600 μs, and the reflected power only rose to a maximum at 40 kW (4%) at the transition. Were the tuner currents at zero, the reflected power would have reached approximately 150 kW. The FFT system has been demonstrated to maintain the matching in almost all plasmas in C-Mod (I_p from 0.4 to 1.2 MA and line-averaged density from 0.5 to $3x10^{20}$ m^{-3}), including the special cases such as during the current ramp-up and deuterium pellet injection.

3.2 Performance in ELMy H-mode

The speed of this FFT system is not optimal for plasmas with ELMs, but helps alleviate their effect. A typical ELM on C-Mod plasmas has rising time about ~50-100 μs [27], while the FFT system adjusts its matching once per computation iteration (200 μs). Fig. 4-(a) shows the antenna loading response for a plasma discharge with large ELMs, shown as the fast rise and decay in the D_α signal and the antenna loading. When the FFT computer detects the sudden change of the loading, the power reflection on the matching side can have risen to about 10% to 15%. Fortunately, in one or two iterations, the power

reflection can be pulled back to below 1%. On the other hand, the intrinsic relatively slow matching speed helps prevent the system matching to a fast arc. It is unclear whether the ferrite material itself can be fast enough to respond the rise of ELMs.

3.3 RF power losses in the tuners

One of major concerns on using ferrite tuners on fusion devices are the rf losses: "dynamic loss effect" and "high loss effect."[28]. "Dynamic loss" occurs at any level of rf excitation, but only at relatively low values of bias field [19]. "High loss effect" occurs at any bias field but only at high levels of rf excitation, and nonlinear and anomalous ferrite behavior can occur. In our perpendicular biasing field setup, the dynamic loss effect should be insignificant based on the test result at low power level as long as the operation coil current does not exceed the limit. An important aspect of the C-Mod antennas is their relatively heavy loading resulting in an operating Q ~ 10-20, and relatively low circulating power than the ICRF system in many other devices. However, during the high power operation of the double-stub system, we may have observed the nonlinear high loss effect. In Fig. 5-(a), the traces of circulating power (forward plus reflected power) from directional coupler DCC and DC2 are plotted. In the second H-mode shown in the figure, the circulating power on DC2 was above 6 MW. In Fig. 5-(b), the rf loss as calculated by comparing the net power in DC1, DCC, and DC2 are plotted, which showed a sudden rise of the loss in tuner 1, particularly in the 2nd H-mode period. The fast oscillations seen in the traces may be related to the chaotic reactance fluctuations of the ferrite as expected during high loss operation. In Fig. 5-(c), the forward power (~ 1.5 MW) and reflected power traces from DC1 are plotted. During the high loss period, the feedback system was not able to maintain below 1% reflection coefficient; instead, the reflection coefficient rose to 3% whereas neither tuner current was railed. The

deviation from perfect match may be due to the fact that the computation algorithm is derived from lossless transmission line theory (see Ref. [21]). In this discharge, the rf pulse was terminated by an arc detected by the optical detector on tuner 1. It is unclear whether the arc was related to the potential rf power deposition on the ferrite tiles. In Fig. 6, we show a trend of the rf loss vs. the circulating power based on all FFT discharges in the double-stub configuration. The power loss is insignificant when the circulating power is less than 4 MW (approximately, max voltage of 25 kV on DCC and 30 kV on DC2), but it rises significantly above 4 MW, and ~ 8% losses can occur at 7 MW circulating power. The upgrade to the triple-stub configuration from the double-stub configuration was driven primarily by the concerns on the voltage handling and rf loss at high power. In Fig. 7, we compare the voltage standing wave patterns in the two configurations. By carefully selecting the location and the lengths of stub 3, the voltage in the FFTs of triple-stub configuration is ~ 30% below those in the double-stub configuration at the same net power. The circulating power level, on the other hand, has been lowered to below 4 MW in DC2 even in the discharge achieving the highest net power (1.85 MW, with max voltage at 37 kV on DC3) in H-mode. As a result, we have not observed similar high power losses as shown in Fig. 5 in the upgraded triple-stub configuration.

4. Discussion and Summary

Implementation of a real-time matching system often runs the potential risk of matching to an arc. We have several ways to avoid such events. First, the optical detectors on the tuners are independent of the matching, and they have been shown to be reliable and effective. Secondly, the FFT range is limited as shown in Fig. 2. If the arc induces a Γ outside the 25% matching region and the arc event is fast than ~200 μs, the arc protection

at DC1, based on the ratio of reflected power and forward power, will protect the FFT system and the antenna. Thirdly, we retain our comprehensive arc detection network in use with the FFT system. To avoid so called slow arc event (> 1 ms), we have arc detection using current probes on the antenna (low voltage locations) based on strap phase/amplitude balance, and this is the primary protection against arcs developing at low voltage locations that have occurred on other devices.

Looking towards future devices like ITER, an FFT network in conjunction with conjugate-T network could enable and maintain maximum power transfer to the plasma throughout the plasma discharge. The system here is a prototype and some of its limitations have been explored, particularly the speed and rf losses. The speed of the system to respond to the load variations could be increased further with a larger power supply and faster computational speed. It is unclear at this time whether an ELM could be tracked exactly but this FFT system, with its limitations, moderates the reflected power excursion below 10%; thus the generator is essentially isolated from the plasma load.

In summary, we have successfully implemented a triple-stub real-time fast ferrite tuning system on one of the ICRF antennas in the Alcator C-Mod tokamak. The system has been able to handle up to 1.85 MW net power into H-mode plasmas, and maintain 1% power reflection in a large range of plasma parameters. It also helps alleviate the effect of ELMs. Similar FFT systems are being considered on other ICRF antennas on Alcator C-Mod.

Acknowledgments

References

[1] R.I. Pinsker, Development of Impedance Matching Technologies for ICRF Antenna Arrays, Plasma Phys. Control. Fusion **40** (1998), A215.

[2] T. J. Wade, J. Jaquinot, G. Bosia, A. Sibley and M. Schmid, Development of the JET ICRH plant, Fusion Eng. Design **24** (1994) 23-46.

[3] G. L. Campbell, J. R. Ferron , E. McKee, A. Nerem, T. Smith, E. A. Lazarus, C. M. Greenfield and R. I. Pinsker 1993 Fusion Technology 1992 (Amsterdam: Elsevier) p 1017

[4] A. Kaye, V. Bhatanagar, P. Crawley, C. Gormezano and J. Jacquinot, The JET wideband matching system, in: P. M. Ryan, et al. (Eds.), 12th Top. Conference on Radio Frequency Power in Plasmas, AIP Conference Proceedings **403** (1997) 389.

[5] G. Bosia, High-power density ion cyclotron antennas for next step applications, Fusion Science Tech. **43** (2003) 153–160.

[6] F. Durodi´e, A. Messiaen, M. Vervier, S. Brons, P. Dumortier, R. Koch, et al., Development of a load-insensitive ICRH antenna system on TEXTOR, Fusion Eng. Design **66–68** (2003) 509–513.

[7] A. Messiaen, M. Vervier, P. Dumortier, P. Lamalle and F. Louche, Study of ITER ICRF system with external matching by means of a mock-up loaded by a variable water load, Nucl. Fusion **46**(2006) S514-S539.

[8] K. Saito, R. Kumazawa, C. Takahahi, M. Yokota, H. Takeuchi, T, Mutah, et al, Real-time impedance matching system using liquid stub tuners in ICRF heating, Fusion Engineering and Design **81** (2006) 2837-2842.

[9] G. Nomura, M. Yokota, R. Kumazawa, C. Takahashi, Y. Torii, K. Saito, et al., Feedback control impedance matching system using liquid stub tuner for ion cyclotron heating, in: T.K. Mau, et al. (Eds.), 14th Top. Conference on Radio Frequency Power in Plasmas, AIP Conference Proceedings, vol. **595**, Oxnard, AIP, 2001, pp. 502–505.

[10] C. M. Qin, Y. P. Zhao, Y. Z. Mao, J. Y. Din, P. Wang, Y. P. Pan, et al., Design of a new type of stub tuner in ICRF experiment, Plasma Science and Technology **3** (2003), 1779–1784.

[11] J.-M. Noterdaeme, Vl. V. Bobkov, S. Bremond, A. Parisot, I. Monakhov, B. Beaumont, et al., Matching to ELMy plasmas in the ICRF domain, Fusion Eng. Design **74** (2005), 191-198.

[12] A. Parisot, S.J. Wukitch, P.T. Bonoli, J.W. Hughes, B. LaBombard, Y. Lin, R. Parker, M. Porkolab, and A.K. Ram, "ICRF Loading Studies on Alcator C-Mod," Plasma Phys. Control. Fusion **46** (2004), 1781.

[13] A. Parisot, S. Wukitch, Y. Lin et al., 31st EPS Conference on Plasma Physics (ECA), 28G, P-2.168 (2004).

[14] E. S. Marmar, The Alcator C-Mod Program, Fusion Sci. and Tech. **51** (2007) 261.

[15] D. B. Remsen, D. A. Phelps, J. S. deGrassie, W. P. Cary, R. I. Pinsker, C. P. Moeller, et al., Feedback controlled hybrid fast ferrite tuners, Proceedings of 15th IEEE/NPSS Symposium on Fusion Engineering, Vol 2, IEEE 1993, p1088.

[16] F. Braun, F. Hofmeister, F. Wesner, W. Beck, H. Faugel, and D. Hartmanm, ICRF system enhancements at ASDEX upgrade, Fusion Eng. Design **56-57** (2001) 551-555.

[17] S. Martin, W. Arnold, E. Pivit, A fast double mode tuner for antenna matching, in: D. Batchelor (Ed.), 9th Top. Conference on RF Power in Plasmas, AIP Conference Proceedings **244** (1992), pp. 318–321.

[18] F. Braun, and W. Arnold, Fast matching of load changes in the ion cyclotron resonance frequency range, in: 18th Symposium on Fusion Engineering, Albuquerque, NM, IEEE, 1999, pp. 395–398.

[19] S. J. Wang and B. G. Hong, Development of Fast Ferrite Tuner for ICRF Experiment in KSTAR Tokamak, Journal of the Korean Physical Society **49** (2006), S302-S304.

[20] P. T. Bonoli, R. Parker, S. J. Wukitch, Y. Lin, M. Porkolab, J. C. Wright, et al., Wave-particle studies in the ion cyclotron and lower hybrid ranges of frequencies in Alcator C-Mod, Fusion Science and Tech. **51** (2007) 401.

[21] Y. Lin, J. A. Stillerman, A. Binus, A. Parisot, and S. Wukitch, Digital real-time control for an ICRF fast ferrite tuning system on Alcator C-Mod, Fusion Eng. and Design **83** (2008) 241-244.

[22] Y. Lin, A. Binus, A. Parisot, and S. Wukitch, Fast Ferrite ICRF Matching System on Alcator C-Mod, in: P.M. Ryan, et al. (Eds), 17th Top. Conference on Radio Frequency Power in Plasmas, AIP Conference Proceedings **933**, 2007, p187.

[23] R. E. Collin, Foundations of Microwave Engineering, 2nd edition, Chapter 5, McGraw-Hill series in electrical engineering, McGraw-Hill, New York, 1992.

[24] J. A. Stillerman, M. Ferrara, T. W. Fredian and S. Wolfe, Digital real-time plasma control system for Alcator C-Mod, Fusion Eng. Design **81** (2006) 1905-1910.

[25] J. A. Stillerman, T. W. Fredian, K. A. Klare and G. Manduch, MDSplus data acquisition system, Review of Scientific Instruments **68** (1997), 939.

[26] M. J. Mayberry, S. C. Chiu, R. I. Pinsker, R. Prater, D. Hoffman, F. W. Baity, et al., Coupling of fast waves in the ion-cyclotron range of frequencies to H-mode plasmas in DIII-D, Nuclear Fusion **30** (1990), 579.

[27] J. L. Terry, I. Cziegler, A. E. Hubbard, J. A. Snipes, J. W. Hughes, M. J. Greenwald, et al., The dynamics and structure of edge-localized-modes in Alcator C-Mod, J. Nucl. Materials 363 (2007), 994-999.

[28] J. E. Griffin and G. Nicholls, A Review of Some Dynamic Loss Properties of Ni-Zn Accelerator RF System Ferrite, IEEE Transactions on Nuclear Science, Vol. NS-26 (1979), No. 3, p3965.

Figure Captions

Figure 1. Layout of the triple-stub fast ferrite tuning system. Ferrite tuners are installed on stub 1 and stub 2. DC1, DCC, DC2 and DC3 are directional couplers. P1 to P6 are transmission line locations shown in Fig. 2.

Figure 2. Triple-stub matching method shown on a Smith Chart in admittance coordinates. Arrows show the transformation path through the system for typical antenna loading. P1 to P6 are labeled on Fig. 1. The solid filled region can be transformed to 50 Ω by the FFT while the line filled region can be transformed power reflection <25% (VSWR < 3).

Figure 3. Performance of the FFT in L-mode and enhanced D_α H-mode. (a) D_α signal and antenna loading. (b) Forward and reflected power traces. (c) Coil currents under real-time feedback.

Figure 4. Performance of the FFT in ELMs. (a) D_α signal and antenna loading with ELMs. (b) Power reflection coefficient as seen by DC1.

Figure 5. RF power loss in the previous double-stub FFT system at high power. (a) Circulating power measured in directional couplers DCC and DC2. (b) Total power loss by comparing DC1 and DC2 net power, and power loss in tuner 1 by comparing DC1 and DCC net power. (c) Forward and reflected power traces from DC1.

Figure 6. RF power loss in double-stub configuration vs. circulating rf power in DC2.

Figure 7. Voltage standing wave patterns on the main transmission line assuming 1 MW net power at typical EDA-H-mode antenna loading: (a) Previous double-stub configuration; (b) Present triple-stub configuration.
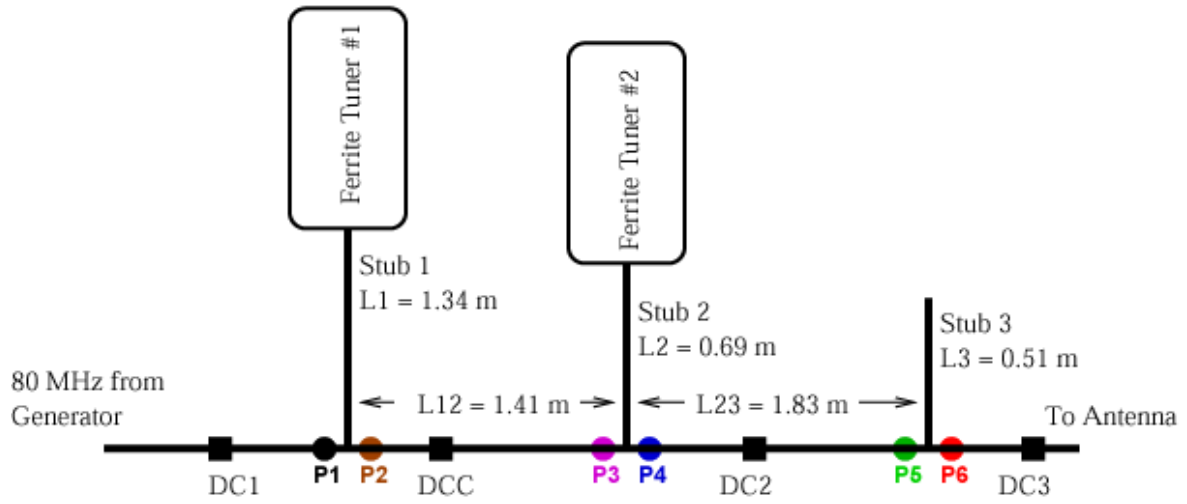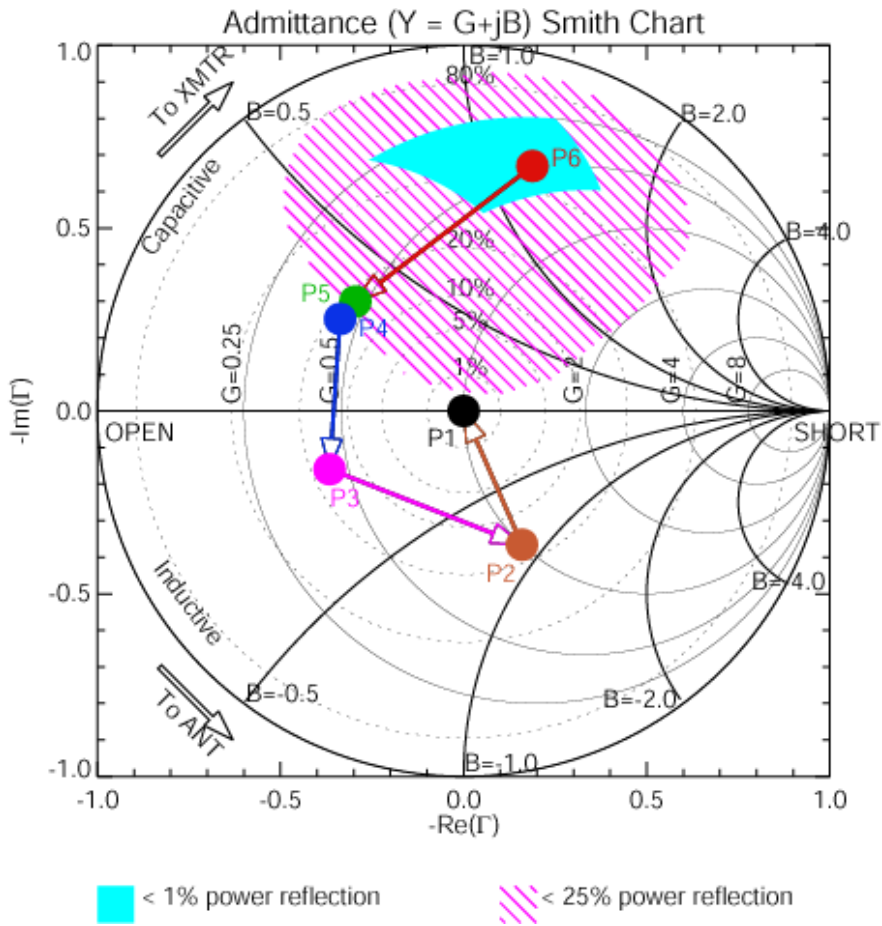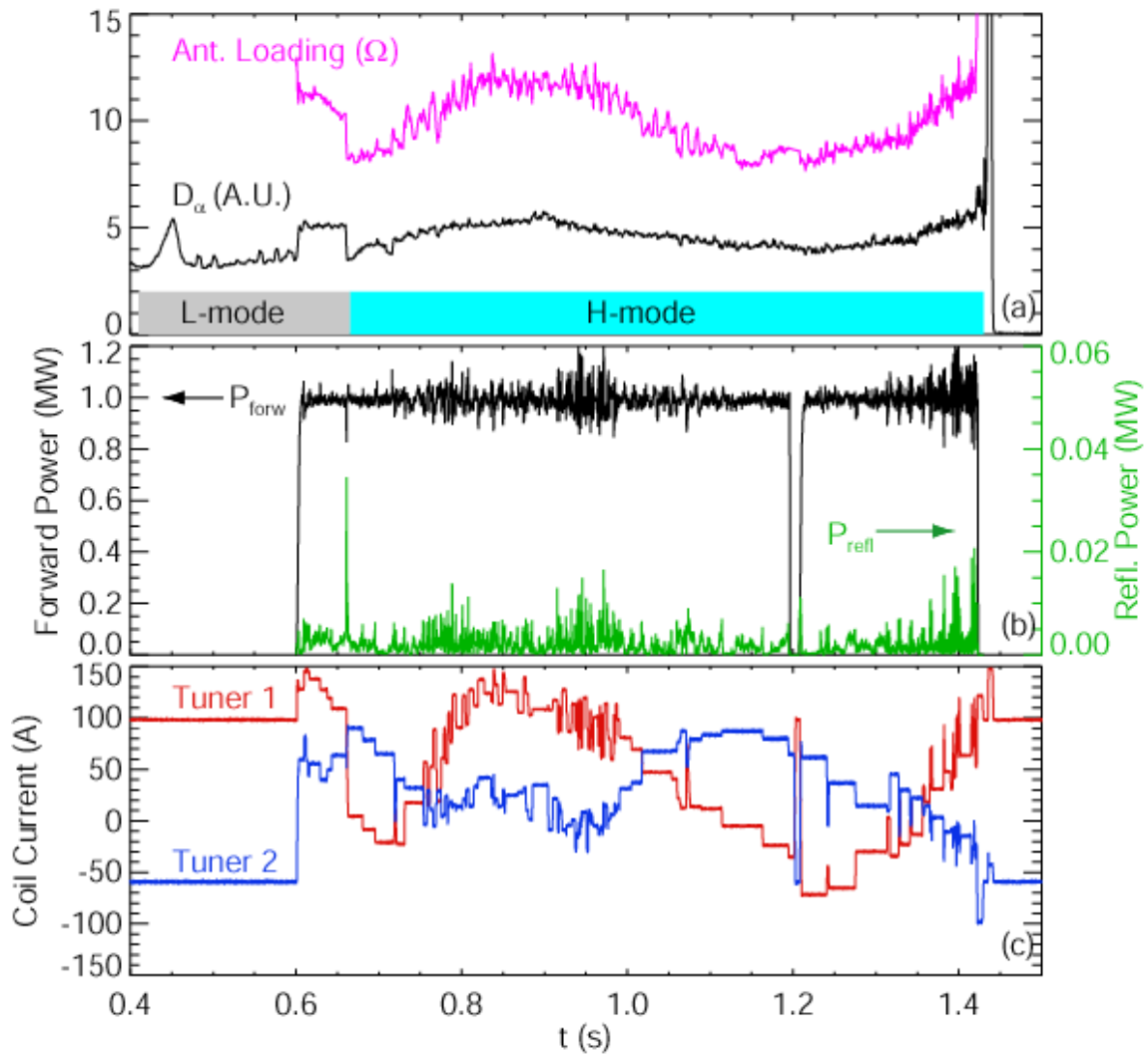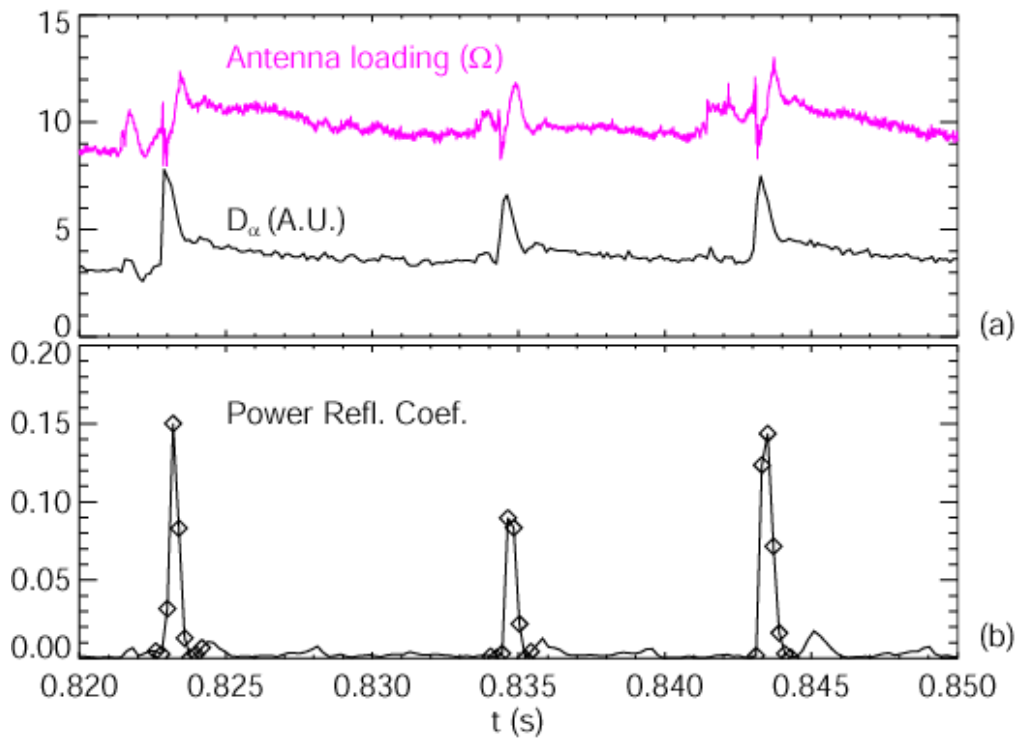
Fig. 1

Fig. 2

Fig. 3

Fig. 4

Fig. 5

Fig. 6

Fig. 7